Original Article
Obstet Gynecol Sci 2022;65(1):52-63
https://doi.org/10.5468/ogs.21237
eISSN 2287-8580

Obstetrics & Gynecology Science

Signature of arylacetamide deacetylase expression is associated with prognosis and immune infiltration in ovarian cancer

Jianyang Feng, MM, Hong He, MD, PhD

Department of Obstetrics and Gynecology, The Third Affiliated Hospital of Guangzhou Medical University, Guangzhou, China

Objective
The role of the protein-coding gene arylacetamide deacetylase (*AADAC*) in the prognostication of ovarian cancer remains uncertain. We aimed to identify and validate its prognostic value using integrated bioinformatics analyses.

Methods
Gene expression profiles of RNA-sequencing and microarray data were retrieved from The Cancer Genome Atlas and Gene Expression Omnibus. Univariate and multivariate Cox regression models were used to evaluate the prognostic value of gene expression. The predictive accuracy of the gene signature model was evaluated using a time-dependent receiver operating characteristic (ROC) curve. In addition, the correlation between immune infiltration and *AADAC* was identified. A nomogram of the gene signature with clinical parameters was constructed to estimate the clinical application of the signature for survival prediction in patients with ovarian cancer.

Results
Univariate and multivariate Cox regression analyses in the training and validation cohorts indicated that a high *AADAC* expression signature was significantly and independently correlated with better survival outcomes in ovarian cancer. *AADAC* upregulation positively correlated with the infiltration of CD4+ memory T cells. Immunological signature gene sets were significantly enriched in CD4+ T cell regulation pathways. The area under the curve of the time-dependent ROC for overall survival indicated that the constructed nomogram had a moderate predictive ability for prognostic prediction in ovarian cancer.

Conclusion
AADAC expression signature significantly and independently correlated with the survival outcome and CD4+ memory T cell infiltration in ovarian cancer, indicating its potential applicability in the prediction of prognosis and immunotherapy efficacy.

Keywords: Arylacetamide deacetylase; Ovarian neoplasms; Computational biology; Tumor microenvironment; Nomogram

Introduction

Ovarian cancer is one of the most fatal malignancies and the leading cause of mortality in cancers associated with the female genital tract, with an estimated 184,799 deaths reported worldwide in 2018 [1]. More than 70% of ovarian cancer cases are diagnosed at an advanced stage and are accompanied by disseminated peritoneal diseases [2]. Distinct molecular phenotypes in ovarian cancer show heterogeneous treatment responses and biological behaviors. For instance,

Received: 2021.07.20. Revised: 2021.10.18. Accepted: 2021.11.02.
Corresponding author: Hong He, MD, PhD
Department of Obstetrics and Gynecology, The Third Affiliated Hospital of Guangzhou Medical University, 63 Duobao Rd, Liwan district, Guangzhou 510000, China
E-mail: hehe2000010@gzhmu.edu.cn
https://orcid.org/0000-0002-5335-5433

although the high-grade serous subtype is more sensitive to chemotherapy, it is also more aggressive than low-grade subtypes. Thus, identification of gene expression signatures with key clinicopathological parameters may facilitate the precise estimation of survival, and consequently lead to the development of personalized treatment strategies. Based on recent advances in genomic sequencing techniques, it is possible to explore the significant genetic variants and expression characteristics of ovarian cancer.

Arylacetamide deacetylase (*AADAC*) is a protein-coding gene located in human chromosome 3. The translated product of *AADAC* competes with cytosolic arylamine N-acetyltransferase activity in the cytochrome P450 pathway and is associated with the biotransformation, hydrolase activity, triglyceride lipase activity, and hydrolysis of clinical drugs [3-5]. *AADAC* is a tissue-specific protein-coding gene that is mainly expressed in normal liver tissues and shows extremely low expression in normal ovarian tissues [6]. However, the role of *AADAC* in the prognostication of ovarian cancer remains inconclusive. Thus, our study aimed to identify and validate the correlation between *AADAC* expression and survival in ovarian cancer cases using integrated bioinformatics analyses. The results of the present study indicated that ovarian cancer cases with high *AADAC* expression signatures were associated with better overall survival. Furthermore, upregulation of *AADAC* was correlated with increased CD4+ memory T cell infiltration in the tumor microenvironment. Finally, by integrating the signature score of *AADAC* expression with clinicopathological parameters, we constructed a nomogram to demonstrate its potential utility in predicting the survival of patients with ovarian cancer.

Materials and methods

1. Acquisition of multi-omics data on ovarian cancer

Gene expression profiles (RNA-sequencing data) of The Cancer Genome Atlas-ovarian cancer (TCGA-OV) cohort were retrieved from TCGA using the University of California, Santa Cruz, Xena browser (USCS Xena) datahub (https://xenabrowser.net/; accessed on October 12, 2020), which is a high-performance visualization and analysis tool for both large public repositories and private datasets [7]. The data included HTSeq-counts and fragments per kilobase of transcript per million values of 379 cases with patient follow-up information. TCGA-OV cohort was used as the training dataset.

Raw microarray data of the GSE18520 and GSE26712 datasets were accessed from the Gene Expression Omnibus (GEO; https://www.ncbi.nlm.nih.gov/geo/). The GSE18520 dataset comprised of gene expression profiles from 53 high-grade primary papillary serous ovarian adenocarcinoma specimens and 10 normal ovarian surface epithelium brushing specimens, which were evaluated using the Affymetrix Human Genome U133 Plus 2.0 Array (Affymetrix, Inc., Santa Clara, CA,USA); while the GSE26712 dataset comprised of 185 primary ovarian tumour samples and 10 normal ovarian surface epithelium samples, which were detected using the Affymetrix Human U133A microarray (Affymetrix, Inc.). For the validation studies, we used the GSE140082 dataset, which comprised of data on the gene expression arrays from 380 formalin-fixed paraffin-embedded ovarian cancer samples and overall survival information of the patients, which was also obtained from the GEO database and evaluated using Illumina HumanHT-12 WG-DASL V4.0 R2 Expression BeadChip Array (GEO; NCBI, Bethesda, MD, USA). Details of the primary data used in this study are presented in Table 1.

Table 1. Characteristic details for the primary dataset

Source	GEO accession	Platform	No. of tumor samples	No. of normal samples	Gene expression profiling	Purpose
TCGA	-	TCGA-OV	379	-	RNA-seq	Training cohort
GEO	GSE140082	GPL14951	380	-	Microarray	Validation cohort
GEO	GSE18520	GPL570	53	10	Microarray	DEA
GEO	GSE26712	GPL96	185	10	Microarray	DEA

GEO, Gene Expression Omnibus; TCGA-OV, The Cancer Genome Atlas-ovarian cancer; DEA, differentially expression analysis.

2. Quality control and processing of the multi-omics data

The quality of the raw data obtained from the GSE18520 and GSE26712 datasets was assessed using the "arrayQualityMetrics" (version 3.44.0; Bioconductor) package [8]. A robust multi-array average algorithm was used for data normalization and background correction. Different microarray scanning times were considered as a known batch effect, which was examined using the ComBat function of the "sva" (version 3.36.0; Bioconductor) package [9]. Batch effect control was performed by using a principal component analysis through the "FaceFactoMineR" (version 2.4; Bioconductor) package [10]. The gene annotation file (gencode.v35.annotation.gtf..gz, https://www.gencodegenes.org/; accessed on October 12, 2020) of the human genome was used to extract data on protein-coding genes and was downloaded from GENCODE (https://www.gencodegenes.org/; accessed on October 12, 2020). Quality annotations of TCGA-OV samples were performed according to the merged_sample_quality_annotations.tsv file (https://gdc.cancer.gov/about-data/publications/pancanatlas). The workflow of the quality control process of TCGA-OV samples is shown in Supplementary Fig. 1. A variance inflation factor was used to detect the severity of multicollinearity between the gene signature and clinicopathological parameters.

3. Differential expression analysis of the protein-coding genes

Differential expression analysis of the protein-coding genes between the normal and cancerous ovarian samples obtained from the GEO datasets was performed using the "limma" (version 3.44.3; Bioconductor) package [11]. The batch effects of the scanning time in the microarray datasets were integrated into the limma model design to conduct further differential expression analysis. Genes with |logFC| >1 and adjusted $P<0.05$, were considered differentially expressed.

4. Identification of survival-associated protein-coding genes

The value of protein-coding gene expression on survival was determined using a univariate Cox proportional hazards model analysis (log-rank $P<0.05$) in the TCGA-OV training cohort.

5. Univariate and multivariate Cox regression model analyses and validation

The intersection data between the potential survival-associated genes and differentially expressed genes were filtered using a least absolute shrinkage and selection operator (LASSO)-penalized Cox regression analysis. Only genes with non-zero coefficients via the minimum criteria (a λ value of 0.066 with log [λ]=-2.718 were selected by a 10-fold cross validation) in the LASSO regression model were chosen to further estimate the prognostic significance using univariate and multivariate Cox regression analyses. Next, Kaplan-Meier survival curves were plotted and the log-rank method was used to estimate the prognostic significance. The signature score of a specific gene was calculated by multiplying the gene expression values by the coefficients. A time-dependent receiver operating characteristic (ROC) curve was plotted to investigate the predictive accuracy using the "survivalROC" (version 1.0.3; CRAN) package [12]. Finally, the validation cohort GSE140082 was used to verify the prognostic significance of the gene signature.

6. Estimation of immune infiltration and immunological signature gene set enrichment in ovarian cancer

xCell [13], a webtool and gene signature-based method was used to perform cell type enrichment analysis based on the gene expression data of 64 immune and stromal cell types. Data on immunological signature gene sets, which represent the cellular states and perturbations within the immune system, were downloaded from the Molecular Signatures Database v7.2 (MSigDB), Broad Institute (https://www.gsea-msigdb.org/; accessed on October 12, 2020).

7. Construction of the nomogram for the gene signature

In the TCGA-OV cohort, the following parameters were selected to construct a nomogram using the "survival" (version 3.2-10; CRAN) [14] and "rms" (version 6.1-1; CRAN) packages: age, stage, grade, and residual disease along with the gene signature score [15]. Calibration curves were plotted to assess the concordance between the actual and predicted survival. A time-dependent ROC curve was plotted to investigate the predictive accuracy of the nomogram.

8. Statistical analysis

An adjusted *P*-value <0.05, with |logFC| >1, was considered significant for differential gene expression analysis. The Kaplan-Meier method and log-rank test were used to estimate the impact of the gene signature on survival. Statistical significance was set at *P*<0.05. A significant Spearman's correlation coefficient was estimated with a *P*-value <0.05. All data were processed using the R software (version 4.0.2 [×64]; R-project) platform.

Results

1. Clinicopathologic characteristics in the training and validation cohorts

The clinicopathologic characteristics (including age, stage, grade, residual disease, and/or debulking surgery) of the training and validation cohorts are summarized in Table 2.

2. Differentially expressed protein-coding genes in ovarian cancer

Normal ovarian samples and ovarian cancer samples from the GSE18520 and GSE26712 datasets were compared according to the adjusted *P*-value <0.05, and |logFC| >1. The batch effect, which was the scanning time in the two microarray profiles, was integrated into the differential expression analysis model and visualized using principal component analysis (Fig. 1D, E, respectively). In the GSE18520 dataset, 1,226 and 712 protein-coding genes were significantly upregulated and downregulated, while in the GSE26712 dataset, 552 and 765 protein-coding genes were upregulated and downregulated, respectively. Volcano plots of the differentially expressed genes are shown in Fig. 1A. Based on the data of these genes, an intersection of 502 differentially expressed (227 upregulated and 275 downregulated) protein-coding genes was observed, and these genes were selected for further analysis (Fig. 1B, C).

3. Survival-related differentially expressed protein-coding genes in ovarian cancer

The correlation between the differentially expressed protein-coding genes and survival in the TCGA-OV cohort was analyzed using a univariate Cox regression analysis (*P*<0.05). A total of 1,354 protein-coding genes were significantly associated with survival in ovarian cancer, and 32 intersecting protein-coding genes from TCGA-OV, GSE18520, and GSE26712 datasets were screened for prognostic value in ovarian cancer (Fig. 1F). Furthermore, data on these 32 genes were filtered using the LASSO-penalised Cox regression analysis (Fig. 1G, H). Moreover, seven genes, including isocitrate dehydrogenase (*IDH2*), FA complementation group I (*FANCI*), C-X-C motif chemokine receptor 4 (*CXCR4*), PRAME nuclear

Table 2. Clinicopathologic characteristics of the training and validation cohort in ovarian cancer

	Training cohort	Validation cohort
Total No. of patients	304	380
Age (yr)	59.5 (30-87)	59 (21-80)
Stage		
II	16 (5.26)	
III	242 (79.61)	
IV	44 (14.47)	
Unknown	2 (0.66)	
FIGO stage		
I		20 (5.26)
II		31 (8.16)
III		266 (70.00)
IV		63 (16.58)
Grade		
G2	26 (8.55)	
G3	269 (88.49)	
Low		74 (19.47)
High		281 (73.95)
Unknown	9 (2.96)	25 (6.58)
Residual disease		
NMD	55 (18.09)	
1-10 mm	141 (46.38)	
11-20 mm	19 (6.25)	
>20 mm	55 (18.09)	
Unknown	34 (11.18)	
Debulking surgery		
Optimal		290 (76.32)
Sub-optimal		88 (23.16)
Inoperable		2 (0.52)
Median survival time (months)	31.5 (1.0-182.7)	25.7 (0.03-44.2)

Values are presented as number (range) or number (%).
FIGO, The International Federation of Gynecology and Obstetrics; NMD, no macroscopic disease.

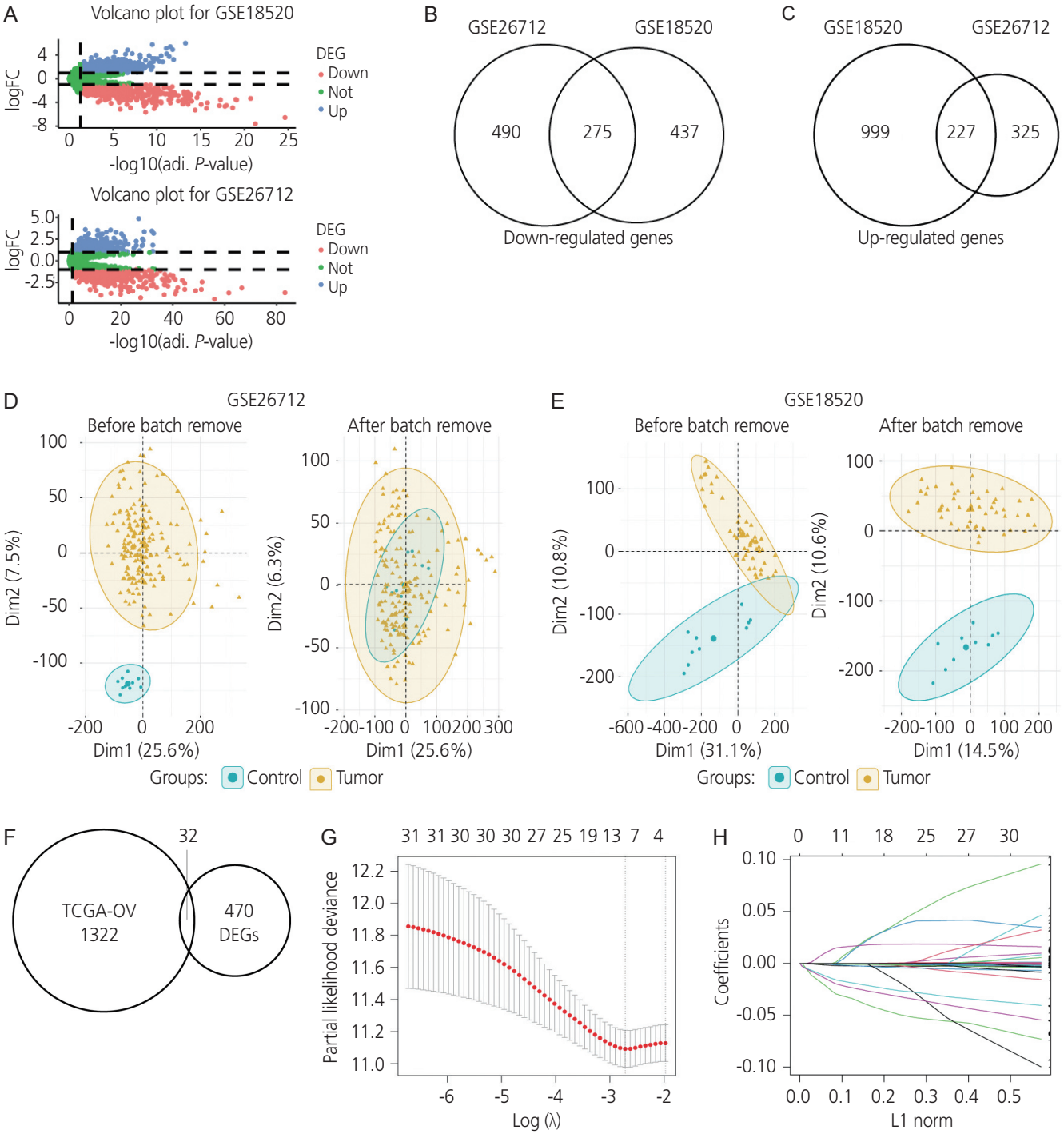

Fig. 1. Differentially expressed protein-coding genes in ovarian cancer. (A) Volcano plots of the differentially expressed genes. (B, C) Intersection of the upregulated and downregulated protein-coding genes in the GSE18520 and GSE26712 datasets. (D, E) Principal component analysis plots for performing the batch effect control. (F-H) LASSO-penalised Cox regression analyses for differentially expressed and survival-related protein-coding genes. DEG, differentially expressed gene; LASSO, least absolute shrinkage and selection operator; TCGA-OV, The Cancer Genome Atlas-ovarian cancer.

receptor transcriptional regulator (*PRAME*), praja ring finger ubiquitin ligase 2 (*PJA2*), enoyl-CoA delta isomerase 2 (*ECI2*), and *AADAC*, were identified for conducting further univariate and multivariate Cox regression validation analyses. Finally, univariate and multivariate Cox proportional hazard regression analyses performed using both the training and validation cohorts verified that *AADAC* was significantly and independently correlated with prognosis in ovarian cancer (Table 3, Fig. 2).

4. AADAC expression signature is associated with prognosis in ovarian cancer

The samples were classified according to the median *AADAC* expression score then grouped as high -and low-score

Table 3. Univariate cox analysis of the protein-coding genes

Gene	Training cohort				Validation cohort			
	β	HR (95%CI)	Wald test	*P*-value	β	HR (95%CI)	Wald test	*P*-value
IDH2	-0.005	0.995 (0.991-0.999)	5.60	0.018	-0.323	0.724 (0.470-1.115)	2.15	0.143
FANCI	-0.089	0.915 (0.857-0.976)	7.25	0.007	0.027	1.027 (0.801-1.317)	0.04	0.833
CXCR4	-0.005	0.995 (0.991-0.998)	7.38	0.007	-0.403	0.668 (0.456-0.979)	4.28	0.039
PRAME	-0.007	0.993 (0.986-1.000)	3.66	0.056	0.021	1.022 (0.924-1.129)	0.17	0.678
PJA2	0.042	1.043 (1.014-1.073)	8.66	0.003	0.286	1.331 (1.026-1.726)	4.63	0.032
ECI2	-0.054	0.948 (0.912-0.985)	7.62	0.006	Not available	Not available	Not available	Not available
AADAC	-0.065	0.937 (0.892-0.984)	6.72	0.010	-0.383	0.682 (0.525-0.885)	8.27	0.004

HR, hazard ratio; CI, confidence interval; *IDH2, isocitrate dehydrogenase; FANCI*, FA complementation group I; *CXCR4*, C-X-C motif chemokine receptor 4; *PRAME*, PRAME nuclear receptor transcriptional regulator; *PJA2*, praja ring finger ubiquitin ligase 2; *ECI2*, enoyl-CoA delta isomerase 2; *AADAC*, arylacetamide deacetylase.

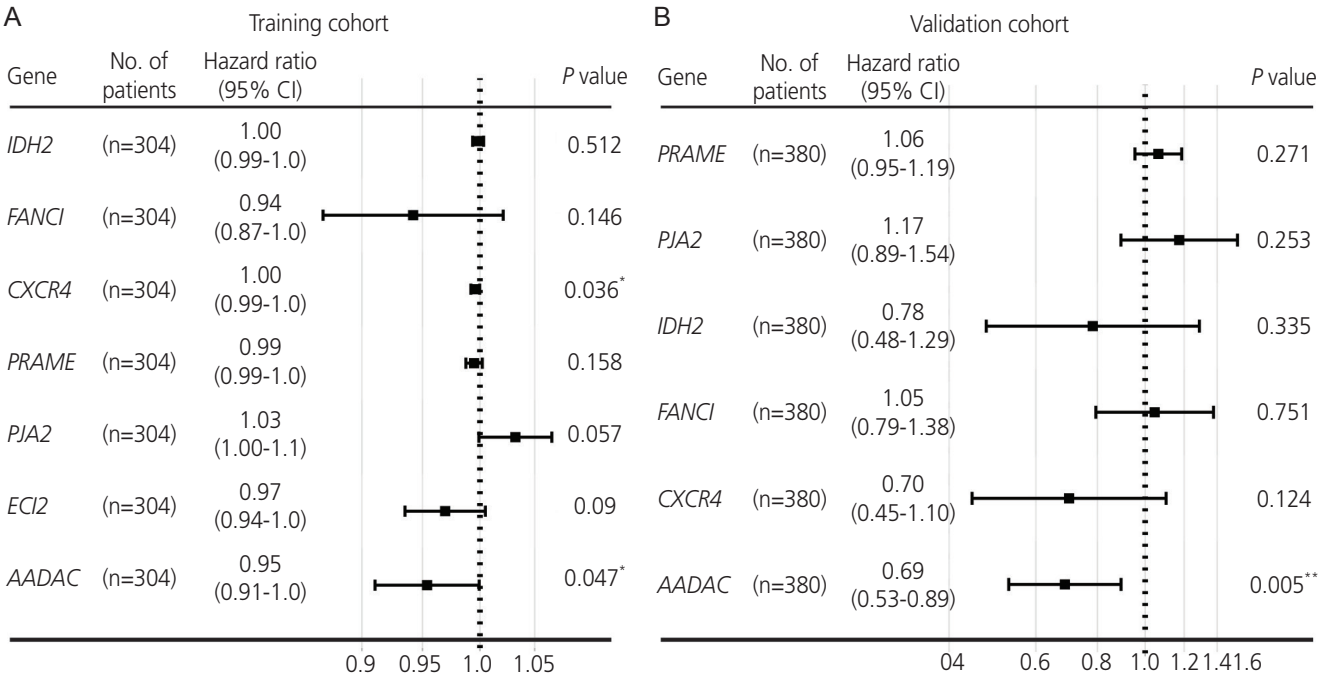

Fig. 2. Univariate and multivariate Cox regression analyses in (A) the training and (B) validation cohorts. CI, confidence interval; *IDH2*, *isocitrate dehydrogenase*; *FANCI*, FA complementation group I; *CXCR4*, C-X-C motif chemokine receptor 4; *PRAME*, PRAME nuclear receptor transcriptional regulator; *PJA2*, praja ring finger ubiquitin ligase 2; *ECI2*, enoyl-CoA delta isomerase 2; *AADAC*, arylacetamide deacetylase. **P*<0.05, ***P*<0.01.

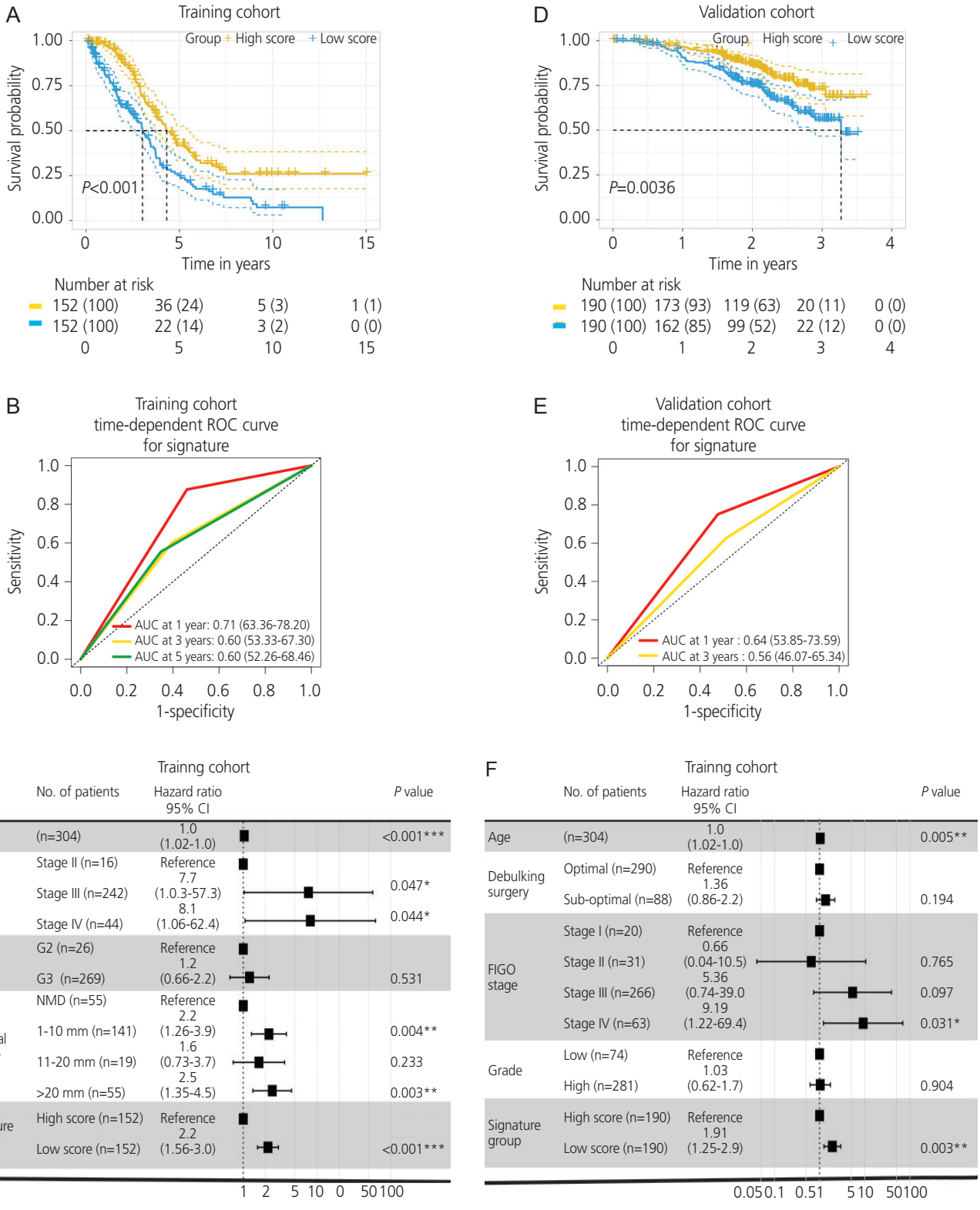

Fig. 3. Kaplan-Meier plot and evaluation of the arylacetamide deacetylase (*AADAC*) signature score in ovarian cancer. (A, D) Kaplan-Meier plot of the *AADAC* signature score in the training and validation cohorts. (B, E) Time-dependent ROC curve of the *AADAC* signature score. (C, F) Multivariate Cox regression analysis of the *AADAC* signature score. ROC, receiver operating characteristic; CI, confidence interval; FIGO, The International Federation of Gynecology and Obstetrics. **P*<0.05, ***P*<0.01, ****P*<0.001.

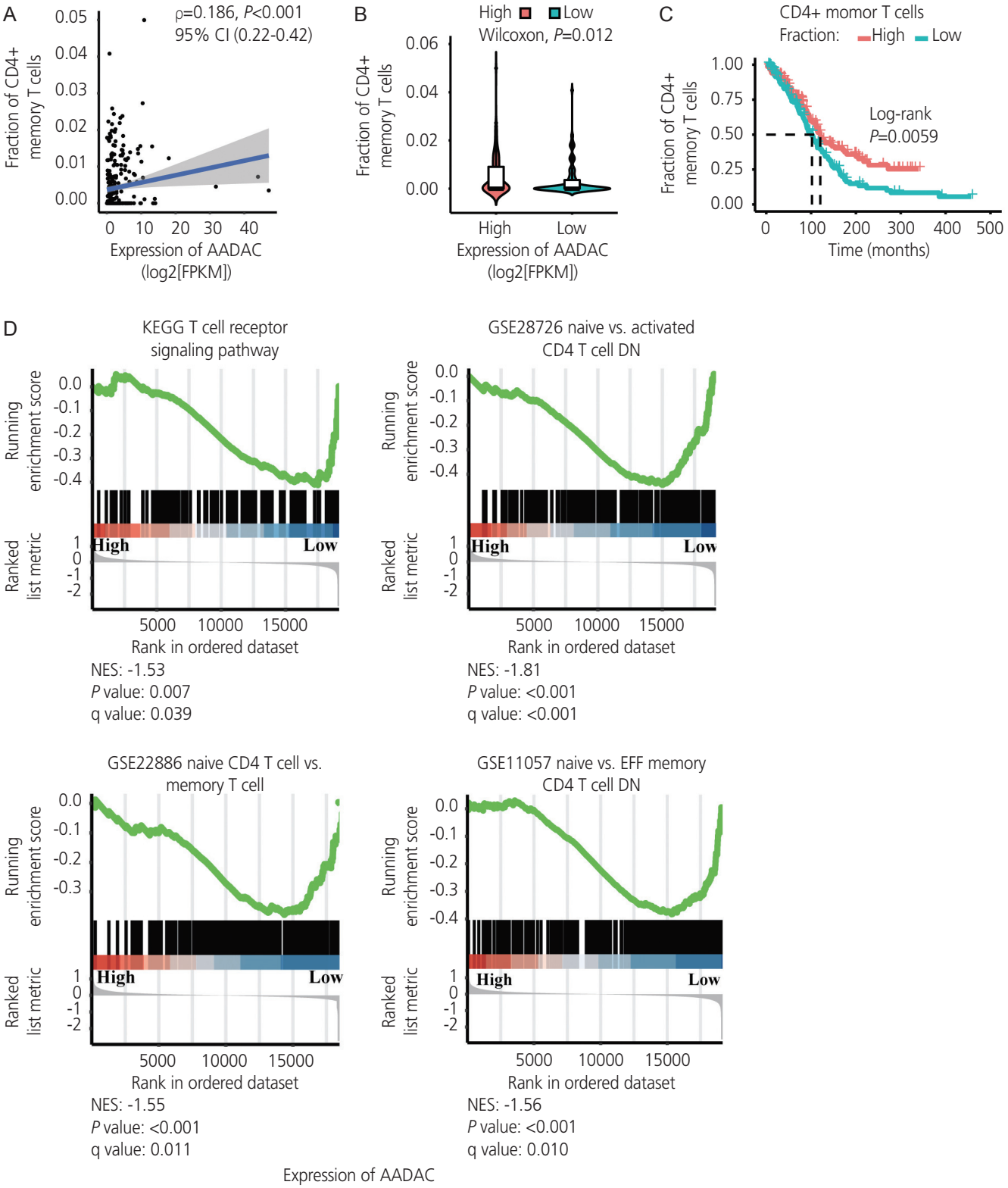

Fig. 4. Correlation of the arylacetamide deacetylase (*AADAC*) expression with immune infiltration and immunological signature in ovarian cancer. (A, B) An increased extent of CD4+ memory T cell infiltration was significantly correlated with the upregulation of *AADAC*. (C) Kaplan-Meier plot illustrating CD4+ memory T cell infiltration. (D) CD4+ T cell enrichment analysis in the immunological signature. CI, confidence interval; NES, normalized enrichment score.

signature groups. The Kaplan-Meier analysis revealed a significant difference in the outcome of the patients with ovarian cancer between the high- and low-score signature groups (log-rank test $P<0.05$; Fig. 3A, D). A better survival outcome was significantly correlated with the high-score *AADAC* expression signature in the subgroup analysis (Fig. 3C, F). The time-dependent area under the ROC curves (AUC) for 1-, 3-, and 5-year survival in the training and validation cohorts are illustrated in Fig. 3B, E, respectively. After combining the *AADAC* signature score with the clinicopathological parameters (age, stage, grade, residual disease, and/or debulking surgery) in both cohorts, multivariate Cox regression and subgroup analyses were conducted, which further indicated that the high-score *AADAC* expression signature was significantly and independently correlated with favorable prognosis in ovarian cancer (Fig. 3C, F). The evaluation of the variance inflation factor suggested that the *AADAC* expression signature showed less collinearity with the other clinical variables in the model (Supplementary Fig. 2). In order to illustrate the reliability of the signature, we sudivided the groups based on the upper and lower quantiles of the *AADAC* expression signature score into the following: top 25%, bottom 25%, and 25-75% subgroups, and the results still demonstrated a favorable prognosis in the top 25% high-score subgroup (Supplementary Fig. 3).

5. Immune infiltration and immunological signature enrichment in ovarian cancer

Immune infiltration in ovarian cancer was estimated using the xCell algorithm. We found that an increased extent of CD4+ memory T cell infiltration was significantly correlated with the upregulation of *AADAC* ($\rho=0.18$; $P<0.001$; 95% confidence interval [CI], 0.22-0.42; Fig 4A, B), and was associated with a better survival outcome (Fig. 4C). Furthermore, the immunological signature enrichment analysis demonstrated that upregulated *AADAC* expression was significantly enriched in genes that were overexpressed in the T cell receptor pathway and CD4+ T cell regulation (Fig. 4D).

6. Nomogram model for the AADAC expression signature with clinicopathologic parameters based on TCGA-OV cohort

We combined the *AADAC* expression signature score with feasible clinicopathologic parameters, including age, stage, grade, residual disease, and signature score (Fig. 5A). Each patient was assigned one point for each prognostic param-

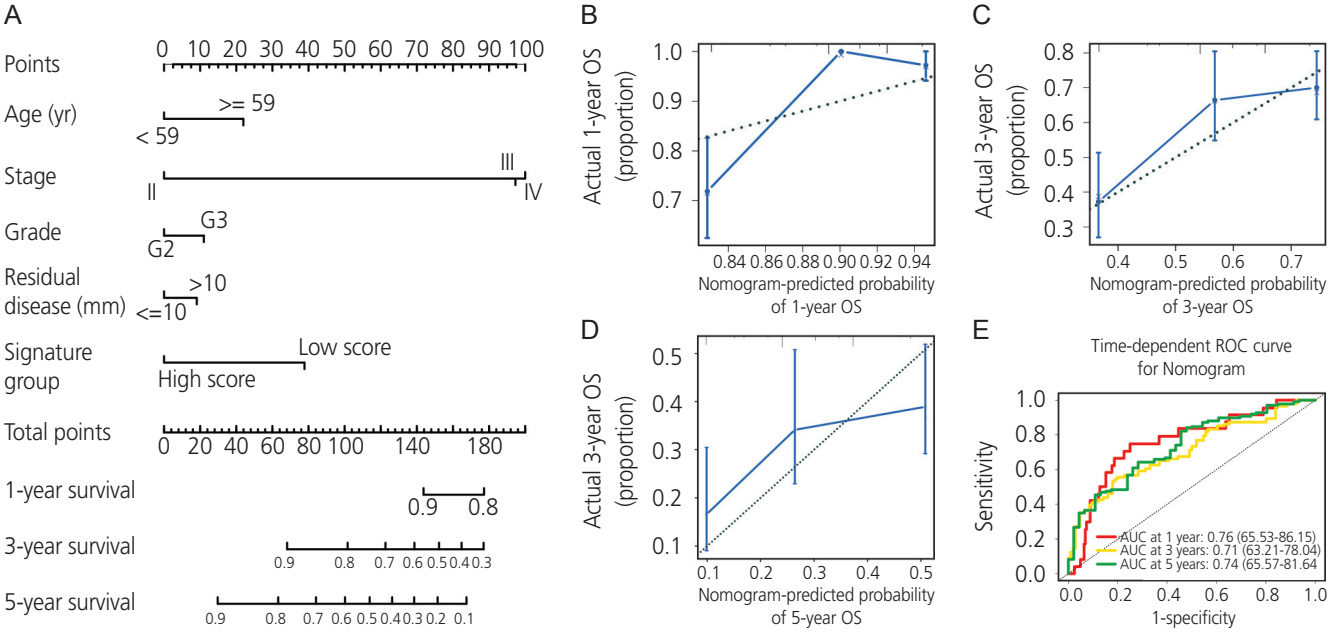

Fig. 5. Nomogram model and evaluation of the arylacetamide deacetylase (*AADAC*) expression signature with clinicopathologic parameters in ovarian cancer. (A) Nomogram model of the *AADAC* expression signature with clinicopathologic parameters. (B-D) Calibration curves of the nomogram model for 1-, 3-, and 5-year survival. (E) Time-dependent ROC curves of the nomogram model for 1-, 3-, and 5-year survival. OS, overall survival; ROC, receiver operating characteristic.

eter: the higher the total number of points, the poorer the outcome. The calibration plots of the nomogram and an ideal model were compared; the nomogram showed moderate performance (Fig. 5B-D). Moreover, the time-dependent AUC of 1-, 3-, and 5-year overall survival demonstrated that our model had a moderate predictive ability (Fig. 5E).

Discussion

Ovarian cancer is the most fatal malignancy associated with the female genital tract [2,16]. Most patients are diagnosed at an advanced stage with early peritoneal dissemination at the primary diagnosis. Patients encounter a disastrous relapse even after undergoing primary debulking cytoreduction surgery and adjuvant platinum-based chemotherapy [16]. Exploration of the significant gene expression characteristics in cancerous samples can directly indicate the inherent molecular heterogeneity in ovarian cancer cells [17-19]. With the development and advancement of multiple "omics" sequencing techniques, the processing of considerable and complex sequencing data using comprehensive and integrated bioinformatics methodologies can help us better understand the underlying molecular characteristics of the cancer genome. In this study, we utilized bioinformatics approaches to estimate the prognostic impact of *AADAC* in ovarian cancer.

AADAC is a tissue-specific protein-coding gene in humans [5] that is highly expressed in the liver but not in the ovarian tissues [3,5,6]. The translated product of *AADAC* participates in various activities related to enzymatic bioactivation reactions [5,20]. Jiang et al. [21] demonstrated that intestinal *AADAC* is involved in vicagrel hydrolytic bioactivation to further influence platelet function. The platelet-lymphocyte ratio has been associated with survival outcomes in various cancer subtypes [22-24]. Recently, Toyohara et al.[25] found that elevated *AADAC* expression in vascular smooth muscle cells was correlated with cell proliferation, migration, and apoptosis.

In the present study, univariate and multivariate Cox regression analysis results indicated that *AADAC* overexpression was significantly associated with better survival in patients with ovarian cancer. Furthermore, survival analysis revealed that, compared with a low-score signature, a high-score signature of *AADAC* expression was significantly and independently related to better outcomes in patients with ovarian cancer. Similarly, Liu et al. [26] suggested *AADAC* expression (hazard ratio, 1.112; 95% CI, 1.042-1.186) as a prognostic gene signature with applicability in predicting the overall survival in gastric cancer via an integrated analysis of multiple gene expression profiles. Finally, we constructed a nomogram based on TCGA-OV cohort and clinicopathologic parameters, including the signature score of *AADAC* expression, age at diagnosis, tumor grade, tumor stage, and residual disease status. The nomogram constructed in the present study demonstrated a moderate potential for predicting ovarian cancer prognosis in clinical practice.

Immune infiltration is highly heterogeneous in ovarian cancer [27,28]. The T cell population participates in the elicitation of an anti-tumor immune response and is associated with survival outcomes in patients with ovarian cancer [29,30]. Similar to the findings of a previous study [30], we observed that a lack of CD4+ memory T cell infiltration in the tumor microenvironment was significantly correlated with a worse outcome. The results indicated that tumor infiltration by the T cell population reflected a tumor-related immune response. Thus, reversal of the immunosuppressive tumor microenvironment provides the possibility of adopting immunotherapy strategies for ovarian cancer treatment.

The limitations of our study must be acknowledged. First, our study lacked the experimental data necessary to validate the findings derived from the bioinformatics analyses. Second, the mechanisms underlying the regulation of *AADAC* expression, as underlined in the comprehensive molecular network, should be further explored. In summary, we identified and validated the correlation between the *AADAC* expression signature and survival outcome in ovarian cancer, highlighting its potential prognostic value. However, future research is warranted to validate these findings. The *AADAC* expression was integrated with age, tumor grade, tumor stage, and residual disease in clinical practice based on the model assessment performed herein; consequently, this might promote the stratification of survival prediction in ovarian cancer. Finally, upregulated *AADAC* expression was correlated with CD4+ T cell infiltration and regulation, processes that participate in the development of adaptive antitumor immunity in the ovarian cancer microenvironment, thereby suggesting its potential utility in the prediction of immunotherapy efficacy in ovarian cancer.

In conclusion, the *AADAC* expression signature was as-

sociated with better survival outcome and demonstrated a favorable prognostic potential for ovarian cancer. Overexpressed *AADAC* correlated with an increased extent of CD4+ memory T cell immune infiltration in the tumor microenvironment. Thus, integration of *AADAC* expression with feasible clinicopathological parameters has potential clinical value in the prediction of prognosis and immunotherapy efficacy in ovarian cancer.

Conflict of interest

The authors declare that they have no competing interests.

Ethical approval

Not applicable.

Patient consent

Not applicable.

Funding information

None.

Acknowledgments

We thank Dr. Jianming Zeng (University of Macau), and all the members of his bioinformatics team, biotrainee, for generously sharing their experience and codes. The authors gratefully acknowledge contributions from the TCGA Network, Prof. Winterhoff B. and Stefan Kommoss S. (Mayo Clinic) for providing the publicly available GSE140082, Prof. Birrer MJ (Surgical Oncology Research Labs, Boston) for GSE18520 and GSE26712.

Supplementary material

Supplementary Fig. 1-3 associated with this article can be found online at https://doi.org/10.5468/ogs.21237.

References

1. Bray F, Ferlay J, Soerjomataram I, Siegel RL, Torre LA, Jemal A. Global cancer statistics 2018: GLOBOCAN estimates of incidence and mortality worldwide for 36 cancers in 185 countries. CA Cancer J Clin 2018;68:394-424.
2. Siegel RL, Miller KD, Jemal A. Cancer statistics, 2020. CA Cancer J Clin 2020;70:7-30.
3. Probst MR, Beer M, Beer D, Jenö P, Meyer UA, Gasser R. Human liver arylacetamide deacetylase. Molecular cloning of a novel esterase involved in the metabolic activation of arylamine carcinogens with high sequence similarity to hormone-sensitive lipase. J Biol Chem 1994;269:21650-6.
4. Gaudet P, Livstone MS, Lewis SE, Thomas PD. Phylogenetic-based propagation of functional annotations within the gene ontology consortium. Brief Bioinform 2011;12:449-62.
5. Kobayashi Y, Fukami T, Nakajima A, Watanabe A, Nakajima M, Yokoi T. Species differences in tissue distribution and enzyme activities of arylacetamide deacetylase in human, rat, and mouse. Drug Metab Dispos 2012;40:671-9.
6. Fagerberg L, Hallström BM, Oksvold P, Kampf C, Djureinovic D, Odeberg J, et al. Analysis of the human tissue-specific expression by genome-wide integration of transcriptomics and antibody-based proteomics. Mol Cell Proteomics 2014;13:397-406.
7. Goldman MJ, Craft B, Hastie M, Repečka K, McDade F, Kamath A, et al. Visualizing and interpreting cancer genomics data via the Xena platform. Nat Biotechnol 2020;38:675-8.
8. Kauffmann A, Gentleman R, Huber W. arrayQualityMetrics--a bioconductor package for quality assessment of microarray data. Bioinformatics 2009;25:415-6.
9. Jeffrey TL, Johnson WE, Hilary SP, Elana JF, Andrew EJ, Yuqing Z, et al. Surrogate Variable Analysis [Internet]. Bioconductor; c2020 [cited 2020 Oct 17]. Available from: https://www.bioconductor.org/packages/3.11/bioc/html/sva.html.
10. Lê S, Josse J, Husson F. FactoMineR: an R package for

multivariate analysis. J Stat Softw 2008;25:1-18.
11. Ritchie ME, Phipson B, Wu D, Hu Y, Law CW, Shi W, et al. limma powers differential expression analyses for RNA-sequencing and microarray studies. Nucleic Acids Res 2015;43:e47.
12. Heagerty PJ, Heagerty and packaging by Paramita Saha-Chaudhuri. survivalROC: Time-dependent ROC curve estimation from censored survival data [Internet]. CRAN; c2013 [cited 2013 Jan 13]. Available from: https://cran.r-project.org/web/packages/survivalROC/index.html.
13. Aran D, Hu Z, Butte AJ. xCell: digitally portraying the tissue cellular heterogeneity landscape. Genome Biol 2017;18:220.
14. Therneau TM, Lumley T, Elizabeth A, Cynthia C. survival: Survival Analysis [Internet]. CRAN; c2021 [cited 2021 Mar 16]. Available from: https://mran.microsoft.com/web/packages/survival/index.html.
15. Harrell FE Jr. rms: Regression Modeling Strategies [Internet]. CRAN; c2021 [cited 2021 Feb 06]. Available from: https://CRAN.R-project.org/package=rms.
16. Berek JS, Kehoe ST, Kumar L, Friedlander M. Cancer of the ovary, fallopian tube, and peritoneum. Int J Gynaecol Obstet 2018;143 Suppl 2:59-78.
17. Tan TZ, Miow QH, Huang RY, Wong MK, Ye J, Lau JA, et al. Functional genomics identifies five distinct molecular subtypes with clinical relevance and pathways for growth control in epithelial ovarian cancer. EMBO MOL MED 2013;5:1051-66.
18. Calura E, Ciciani M, Sambugaro A, Paracchini L, Benvenuto G, Milite S, et al. Transcriptional characterization of stage I epithelial ovarian cancer: a multicentric study. Cells 2019;8:1554.
19. Cancer Genome Atlas Research Network. Integrated genomic analyses of ovarian carcinoma. Nature 2011;474:609-15.
20. Fukami T, Iida A, Konishi K, Nakajima M. Human arylacetamide deacetylase hydrolyzes ketoconazole to trigger hepatocellular toxicity. Biochem Pharmacol 2016;116:153-61.
21. Jiang J, Chen X, Zhong D. Arylacetamide deacetylase is involved in vicagrel bioactivation in humans. Front Pharmacol 2017;8:846.
22. Zhang N, Jiang J, Tang S, Sun G. Redictive value of neutrophil-lymphocyte ratio and platelet-lymphocyte ratio in non-small cell lung cancer patients treated with immune checkpoint inhibitors: a meta-analysis. Int Immunopharmacol 2020;85:106677.
23. Chon S, Lee S, Jeong D, Lim S, Lee K, Shin J. Elevated platelet lymphocyte ratio is a poor prognostic factor in advanced epithelial ovarian cancer. J Gynecol Obstet Hum Reprod 2021;50:101849.
24. Wang H, Ding Y, Li N, Wu L, Gao Y, Xiao C, et al. Prognostic value of neutrophil-lymphocyte ratio, platelet-lymphocyte ratio, and combined neutrophil-lymphocyte ratio and platelet-lymphocyte ratio in stage IV advanced gastric cancer. Front Oncol 2020;10:841.
25. Toyohara T, Roudnicky F, Florido MHC, Nakano T, Yu H, Katsuki S, et al. Patient hiPSCs identify vascular smooth muscle arylacetamide deacetylase as protective against atherosclerosis. Cell Stem Cell 2020;27:178-80.
26. Liu X, Wu J, Zhang D, Bing Z, Tian J, Ni M, et al. Identification of potential key genes associated with the pathogenesis and prognosis of gastric cancer based on integrated bioinformatics analysis. Front Genet 2018;9:265.
27. Zhang AW, McPherson A, Milne K, Kroeger DR, Hamilton PT, Miranda A, et al. Interfaces of malignant and immunologic clonal dynamics in ovarian cancer. Cell 2018;173:1755-69.e22.
28. Jiménez-Sánchez A, Cybulska P, Mager KL, Koplev S, Cast O, Couturier DL, et al. Unraveling tumor-immune heterogeneity in advanced ovarian cancer uncovers immunogenic effect of chemotherapy. Nat Genet 2020;52:582-93.
29. Odunsi K. Immunotherapy in ovarian cancer. Ann Oncol 2017;28(suppl_8):viii1-7.
30. Zhang L, Conejo-Garcia JR, Katsaros D, Gimotty PA, Massobrio M, Regnani G, et al. Intratumoral T cells, recurrence, and survival in epithelial ovarian cancer. N Engl J Med 2003;348:203-13.